Impacts of the Variations of Aerosols Components and Relative Humidity on the Visibility and Particles Size Distribution of the Desert Atmosphere: Validating Results Obtained from OPAC 4.0 using MERRA-2 Model (Angstrom Exponent and Extinction Coefficient) Data

S. U. Yerima [a*], B. I. Tijjani [b] and U. M. Gana [b]

[a] *Nigerian Meteorological Agency (NIMET), Nnamdi Azikwe International Airport, Abuja, Nigeria.*
[b] *Department of Physics, Bayero University Kano, Kano State, Nigeria.*

Authors' contributions

This work was carried out in collaboration among all authors. All authors read and approved the final manuscript.

Original Research Article

ABSTRACT

In this work, data extracted from OPAC 4.0 was compared and validated with 11 years data record from MEERA-2 model (average Angstrom Exponent and average Extinction Coefficient). The 11 years MEERA-2 model data for 10 selected deserts was extracted at an average relative humidity (RH) condition of 78%RH while OPAC considers eight different (RH) levels (00% to 99%RH). Based on the investigation, MEERA-2 model has the highest angstrom exponent (α) values for (Arabian, Danakil, Ferlo, Lompoul, Patagonian, Registan and Syrian deserts), which is greater than 1, and this signifies the dominance of fine mode particles over coarse mode particles when compared to OPAC 4.0. It can be seen that Chalbi (0.845), Karoo (0.482) and Sahara (0.417) deserts have an α values which is less than 1(indicating the dominance of coarse mode particles over fine mode particles). It can also be said that, MEERA-2 (α) is still greater than that of OPAC and this shows that the deserts atmosphere can be dominated by fine mode particles. The angstrom exponent (α)

_____

*Corresponding author: E-mail: sunusiyerima@yahoo.com, Sunusiyerima86@gmail.com;

for OPAC 4.0 fluctuate all through the four studied components except for WASO which increases with the increase in RH and particles concentration (and this signifies that the particles dissolved as they uptake water and reach their saturation level). Based on the results of the investigation (time series analysis), it was found that the model's significance (β) level are very high, and this shows that the aerosols distribution fluctuates around a reasonable stable, which signifies that the models are very significant. The analysis further found that, the significance (δ) from the seasonal aspect is very poor except for Ferlo and Lompoul deserts, this signifies that season effect is consistent over time. It was also found that, the MEERA-2 has the highest visibility (km) over (OPAC 4.0). The investigation further revealed that the Arabian, Syrian and Patagonian deserts have the highest visibility (km) in the months of January, February, June, November and December. OPAC model underestimated the visibility when compared to MEERA-2 model.

1. INTRODUCTION

Dust consists of small solid particles. Dust particles are usually in the size range from about 0.2 to 100 µm in diameter [1], [2]. Dust can be either suspended within the atmosphere as aerosols, or accumulate as sediment on the surface of the Earth [3]. Due to the variety of sources that can give rise to dust, it can be composed of many different substances, both organic and inorganic. Mineral dust pollution occurs in the gaseous form as aerosols [4]. In scientific terms, an aerosol is defined as a system of particles suspended the air. Aerosols may exist in the following forms: airborne dusts, sprays, mists, smokes and fumes [4–6]. all these forms are important because they are associated with the wide range of occupational diseases. Mineral dusts are of particular interest because they are well known to be associated with classical widespread of occupational lung diseases such as the pneumoconiosis, as well as with systemic intoxications such as lead poisoning, especially at higher levels of exposure [2]. But, in the modern era, there is also an increasing interest in other dust-related diseases, such as cancer, asthma, allergic alveolitis, and irritation, as well as a whole range of non-respiratory illnesses, which may occur at much lower exposure levels [6].

World health organization (WHO) considers the impacts of air pollution as a worldwide health emergency need [7]. Natural pollutants from particulate matter is liable for an estimated 1.4% of all mortality rates around the globe [6]. It is well know that particulate matter is also generated from mineral dust [8]. Residue from the Sahara is the biggest source of mineral dust in the atmosphere [8–10]. It is a wonder of interest for meteorological material science as well as for general wellbeing too, because of the potential health effect of its air dispersal and flow in the atmosphere [11], [12].

In the natural environments the changes in the microphysical and optical properties observed at a given wavelength with respect to the corresponding change in relative humidity is a signs that measuring condition have changed [4], [9–11]. These changes can cause unbalance in the atmosphere by causing decrease in visibility or other harmful effects to man and his environment [10]. Many of the papers published to date that provide information on health/environmental related mineral and Saharan dust research have focused on the impact of anthropogenically generated mineral or airborne dust related (such as PM generated by combustion engines) [13], while relatively little work has looked at the impact of variations of the meteorological parameters and micro physical properties of the naturally generated dust (such as all forms of dust emanating from dust storms).

Estimates of the contribution of the different source of the Saharan dust also vary by study and are more difficult to make, especially as each source area follows a distinct seasonal cycle [14]. studies addressing the problems all agree that North Africa is the main source area (over 50 %) as said by [15] and [16]. Regions of the world in the path of dust-laden wind record increased ambient air dust concentrations that are temporally associated with deteriorations in air quality and the strong possibility of negative impacts on human health [16],[17]. Generally speaking, a distinction is made between coarse and fine mode particles [18]. Thus, coarse particles are more likely to be deposited in the bronchial passages and thereby affect respiratory conditions such as asthma, chronic obstructive pulmonary disease (COPD), and pneumonia. In contrast, fine particles seem more

likely to reach the alveoli and lead to cardiovascular events [19]. the theory on mathematically oriented time series analysis is vast and mostly very difficult for non-statisticians to use. Some basic properties of time series process and models are used in this work to visualized and describe time series data, on how to fit models to data correctly and on how to adequately draw the future conclusion from the output that was produced [20].

In this work, average aerosol extinction coefficient and average Angstrom Exponents (α) extracted from MERRA-2 Model data (for 10 selected deserts across the world) at 550nm and an average RH of 78% from 2010 to July 2021 was used to validate results obtained from simulations carried out using OPAC 4.0 in our previous work [10] using time series analysis.

2. DATA AND METHOD

2.1 Theoretical Frame Work

An objective measure of visibility is the standard visual range or meteorological range [21].

$$Vis(\lambda) = \frac{3.912}{\sigma_{ext}(\lambda)} \qquad (1)$$

Meteorological range refers to the visual range of a black object seen against its surrounding [22]. The visual extinction coefficient $\sigma_{ext}(\lambda)$ is the measure of light scattering and absorbing properties of the atmosphere along the line of sight [23]. To determine the visibility using the extracted extinction coefficient, the variation of the extinction coefficient with wavelength was determined using the inverse power law of extinction coefficient as;

$$\sigma_{ext}(\lambda) = \beta\lambda^{-\alpha} \qquad (2)$$

where α and β are known as Angstrom parameters. The index α is the wavelength exponent or Angstrom coefficient and β is the turbidity coefficient representing the amount of aerosols present in the atmosphere in the vertical direction or the total aerosol loading in the atmosphere [24], [25].

Substituting equation (2) into (1), the following equation is obtained which is the variation of the visibility with wavelength.

$$Vis(\lambda) = \frac{3.912}{\beta}\lambda^{\alpha} \qquad (3)$$

Equation (3) can also be written as:

$$ln\left(\frac{Vis_{\lambda}}{3.912}\right) = -ln(\beta) + \alpha\,ln(\lambda) \qquad (4)$$

To obtain α (slope) and β (intercept) a regression analysis was performed using an expression derived from the Kaufman (1993) representation of the equation [26].

2.2 MEERA-2 Model

The MERRA-2 aerosols data collection system is based on the Goddard Earth Observing System Model, Version 5 (GEOS-5) [3]. This particular model is assembled with the GOCART chemistry module which simulates (black carbon, sand dust, organic carbon, sulfate, and sea salt) aerosols type [3]. For aerosol dataset, MEERA-2 model collect aerosol data from ground-based AERONET a and space-borne aerosol products from Advanced Very High-Resolution Radiometer (AVHRR), Multi-angle Imaging Spectro Radiometer (MISR) and MODIS [3]. MERRA-2 aerosol dataset includes the five types of aerosols' optical properties, emissions, deposition, and aerosol mixing ratios, vertically [27]. For example, aerosol optical property products include aerosol extinction optical thickness at 550 nm, aerosol scattering optical thickness at 550 nm and aerosol angstrom exponent (470–870 nm) for total as well as five aerosol components [27]. The temporal and spatial resolution of the data is 0.625 degrees × 0.5 degrees, and there are three temporal resolutions: monthly, hourly and every three hours. In the vertical direction, MERRA-2 aerosol dataset is divided into 72 different layers from surface to 0.01 hPa. MERRA-2 data cover the period from 1980 to the present, and they include 21 types of products, such as atmospheric aerosols, radiation, temperature, water vapor, precipitation etc. In this study, we use the monthly average aerosol component column concentration data product (MERRA-2_400.inst3_3d_aer***) for average angstrom exponent and average total extinction coefficient to validate the data extracted from the OPAC software package.

2.3 The OPAC Software Package

The OPAC programming software comprises of two sections, the initial segment is a dataset of microphysical properties and the subsequent optical properties of cloud and aerosols components at various wavelengths and for

different relative humidity conditions [4], [9–11], [23], [28]. The other part is a FORTRAN program that permits the user to separate information from this dataset, to compute extra optical properties, and to ascertain optical properties of the mixtures of the stored cloud and aerosols components. The dataset gives the microphysical and optical properties for six kinds of water clouds, three ice mists, and 10 aerosols components. the data is accessible at 61 wavelengths in the range of 0.25 and 40 μm for aerosols and clouds, and at 67 wavelengths in the range of 0.28 and 40 μm for ice clouds. The information is given for each case for 1 molecule cm^{-3} which portrays the compelling properties of the combination of all particles in the size distribution. For functional use, the values must be multiplied by the total number density. On account of those aerosols components that can take up water, data for eight values of relative humidities (0%, 50%, 70%, 80%, 90%, 95%, 98%, 99%) are given (Abdulkarim et al. 2021; S. U. Yerima, Abdulkarim, Tijjani, Gana, Sani, Aliyu, et al. 2021; S. U. Yerima, Abdulkarim, Tijjani, Gana, Sani, and Aliyu 2021; S. U. Yerima, Tijjani, and Gana 2021). The information is stored as ASCII files, one record for each cloud or aerosols component and for each relative humidities. The computer code executes two tasks. First, single cloud or aerosols segments can be chosen, and all or a portion of their optical properties can be extracted or determined from the dataset. Second, it is feasible to choose one of those combinations of the aerosol's components, which are proposed as default values in OPAC, or to characterize an extra mixture and to obtain its optical properties [10]. Height placement of aerosols particles is given but may likewise be changed with information given by the user. For versatility, the program is disseminated as FORTRAN source code. All mandatory input to the program must be entered as an ASCII text document [10].

To operate OPAC the following steps are followed:

a. The first step is to choose the desired mixture of aerosols or cloud components.
b. The second step deals with choosing the height profile if you are not using the default mixture (i.e here is where you introduce the new profiles).
c. The third step is where you choose the wavelengths for which you want calculate the optical parameters from the already stored data base.
d. The fourth step deals with choosing the relative humidities range for which the calculations of the selected optical parameters should be made.
e. The fifth step is where you choose the optical parameters.
f. The sixth step is where you compile, build and execute the above selection.
g. The seventh step is where you get the calculated optical properties of clouds or aerosols from the output file.
h. The seventh step is where you get the calculated optical properties of clouds or aerosols from the output file.

2.4 Data Analysis

This work chose MERRA-2 model because one of the driving forces of the GEOS DAS products has historically been temperature and Relative Humidity. But it should be noted that this work did not include temperature components, it only considered atmospheric moisture (relative humidity) part. The work extracted total extinction coefficient and total angstrom exponent data for the period of 10 years and seven months (2010-july, 2021) at 550nm wavelength. The area average time series for Arabian (19.4914° N, 47.4490° E), Ferlo (15.8797° N, 15.2502° W), Lompoul (15.4626° N, 16.6910° W), Syrian (34.3504° N, 38.6600° E), Patagonian (41.3200° S, 69.3201° W), Registan (30.4563° N, 65.4004° E), Sahara (23.4162° N, 25.6628° E), Chalbi (34.6068° N, 49.3286° E), Danakil (11.8764° N, 41.9196° E) and Karoo (32.8146° S, 22.2384° E) deserts was extracted from MEERA-2 respectively. The extracted data was then averaged. The averaged extinction coefficient data at 550nm was then used to calculate the visibility using a relation derived by [26]. The angstrom exponent was also averaged and used to perform a time series analysis on the data for each of the deserts to observe if the model fits the observed data using angstrom exponent (α) level and seasonality effects. The visibility and angstrom exponent computations was also performed on the data extracted from OPAC 4.0 at 550nm for 8 relative humidity's levels (00% to 99%RH) as done in our previous work [10] using time series analysis. The results obtained was then compared and validated using that of MEERA-2.

To analyze the data, time series expert modeler of SPSS 16.0 software was used. The modeler only selects the predictors to find the best model of those predictors that have a statically

significant relationship with the dependent series. It shows how the predictors are useful in terms of how each predictor is significant. The model developed can be used for making forecast with the predictors. An important preliminary step in any data analysis is to consider the possibility of a nonlinear data transformation. It is often the case that the scale in which the data naturally arrives to the data analyst is not necessarily the best scale to analyze the in. the primary goal of the transformation is to identify a scale where the residuals after fitting a model will have homogeneous variability and be independent of the level of the time series. Another is a simplified data structure. The most common transformation used is the logarithmic transformation. The modeler will give either exponential smoothing or ARIMA models. It shows whether the model is additive or multiplicative and whether there is/are transformation [20].

The steps taken in analyzing the OPAC and MERRA-2 data:

a. The visibility was computed using equation (3)
b. A regression analysis was performed using equation 4 to obtain the results used in plotting the visibility for OPAC and that of MEERA-2
c. The visibility for MERRA-2 was also calculate using equation 3 and the downloaded MEERA-2 total extinction coefficient.

3. RESULTS AND DISCUSSIONS

The results obtained from the analysis of both MERRA-2 and OPAC are presented in this section. The obtained results from OPAC models (water soluble WASO, mineral nuclei mode MINN, mineral coarse mode MICN and mineral accumulation mode MIAN) where compared and validated with MEERA-2 model. From the five models studied, models 1 and 5 were considered because all the models change in the same pattern and showed the same mode of distributions. Table 1 shows the result of the time series analysis for the angstrom exponent extracted from MEERA-2 model. It can be seen that the models obtained were all simple season models. These simple season models are appropriate for series with no trend and a seasonal effect that is consistent over time, and the smoothing parameters involved are significance level (β) and season (α). From the

table, it can be seen that the significance for all the levels is very high, and this shows that the aerosols distribution fluctuates around the reasonable mean. However, from the seasonal aspect, it can be seen that the significance is very poor for all the studied deserts except for Ferlo and Lompoul deserts, and this implies that the season effect is constant over time except for the two mentioned deserts above. Now, since it is known from the definition that, stationary R^2 is more preferable when the data has trend or seasonal pattern and R^2 is most useful when the data is stationary, it can be said that Ferlo and Lompoul can be best described by stationary R^2 and the others by R^2. But by comparing R2 and stationary R2, it can be said that the stationary part is captured more than the non-stationary part. By comparing the model's significance of the whole models, it can be seen that only Ferlo and Lompoul have poor significance.

Table 2 presents the average visibility (km) and the Average angstrom exponent from MEERA-2 model. It can be seen that the Arabian, Syrian and Patagonian have the highest visibility (km) over the rest of the deserts throughout the study period. It can also be noted from the α values that all the deserts have an angstrom exponent (α) values above 1 except for Chalbi, Karoo and Sahara and this signifies that Chalbi, Karoo and Sahara deserts atmosphere is dominated by coarse mode particles with some traces of fine mode particles while Arabian, Danakil, Ferlo, Lompoul, Patagonian, Registan and Syrian deserts atmosphere is dominated by fine mode particles with some traces of coarse mode particles. Also, by comparing the average visibility with the average angstrom exponent (α), it can be said that the relationship between the visibility and α doesn't satisfy the direct power relation (equation 4).

3.1 Visibility

Figs. 1a to 1h present the plots of MERRA-2 model computed visibility with that of OPAC for eight RHs (00% to 99%RH). It can be observed that Arabian, Syrian and Patagonian deserts have the highest visibility in the months of January, February, June, November and December respectively. It can also be seen that Ferlo, Lompoul, Registan, Sahara, Chalbi, Danakil and karoo Deserts followed same trend with OPAC models, have almost the same visibility values except that OPAC has higher values of the visibility compared to the MEERA-2 Model for the months of May, June, July, August

and sometimes September respectively. It should also be noted that five OPAC models where considered for this study but only two are presented here (models 1 and 5). Among the four OPACs studied components, water soluble (WASO), Mineral Nuclei mode (MINN) and Mineral coarse Mode (MICN) has the highest visibility values (km) while Mineral Accumulation mode (MIAN) has the least. The visibility decreases with the increase in RH for all the four studied components.

3.2 Angstrom exponent (α) plots

Figs 2a to 2h present the comparison plots of angstrom exponent (α) for both MERRA-2 model and OPAC. It can be seen that Ferlo and Lompoul deserts have the highest α values which is greater than 1 and this signifies that

Ferlo and Lompoul deserts atmosphere are dominated by fine mode particles with some traces of coarse mode particles more than the rest of the studied deserts. it can also be seen that the moths of August, September and November have the highest angstrom exponent (α) values for all the study period. The angstrom exponent (α) for OPAC increases with the increase in relative humidity for all the four studied components. It should also be noted that MIAN has the least α values which signifies the dominance of coarse mode particles with little traces of fine mode particles in the case of MIAN component. In general, α values for the Deserts (MEERA-2 model) are greater than that of OPAC except for Sahara Desert (for the months of May, June, July and August) and Karoo desert (June, July, August, September, October and November).

Table 1. Model statistics and exponential smoothing model parameters from the time series analysis for angstrom exponent

S/N	Deserts	Model	Estimate	Sig.	R^2	Stationary R^2	Model Sig.
1	Arabian	β(level)	0.40000	0.00000	0.75400	0.62800	0.00600
		δ(season)	0.00002	0.99900			
2	Chalbi	β(level)	0.99900	0.00000	0.97400	0.47400	0.00000
		δ(season)	0.00000	1.00000			
3	Danakil	β(level)	0.40000	0.00000	0.66300	0.60700	0.01100
		δ(season)	0.00001	1.00000			
4	Ferlo	β(level)	0.83500	0.00000	0.87200	0.53000	0.11400
		δ(season)	0.36070	0.00000			
5	Karoo	β(level)	0.70000	0.00000	0.80500	0.57200	0.03200
		δ(season)	0.00008	0.99800			
6	Lompoul	β(level)	0.83800	0.00000	0.87400	0.53100	0.19500
		δ(season)	0.36564	0.00000			
7	Registan	β(level)	0.50000	0.00000	0.78000	0.55900	0.00000
		δ(season)	0.00009	0.99600			
8	Sahara	β(level)	0.70000	0.00000	0.84900	0.59600	0.09700
		δ(season)	0.00002	0.99900			
9	Syrian	β(level)	0.50000	0.00000	0.79600	0.50500	0.02400
		δ(season)	0.00001	1.00000			
10	patagonian	β(level)	0.60000	0.00000	0.76200	0.56800	0.23800
		δ(season)	0.00000	1.00000			

Table 2. Average visibility (km) and angstrom exponent (α) for MEERA-2 at 550nm

| S/N	Deserts	Average Visibility (km)	Average Anstrom Exponent (α)
1	Arabian	128.6271661	1.353648112
2	Chalbi	27.58618686	0.844595516
3	Danakil	19.46854585	1.164668588
4	Ferlo	28.11175721	1.515039642
5	Karoo	18.64908207	0.481856832
6	Lompoul	28.76357629	1.504852986
7	Patagonian	77.66958216	1.045684297
8	Registan	27.08996425	1.195060063
9	Sahara	19.04847381	0.41700109
10	Syrian	81.03731911	1.099076596
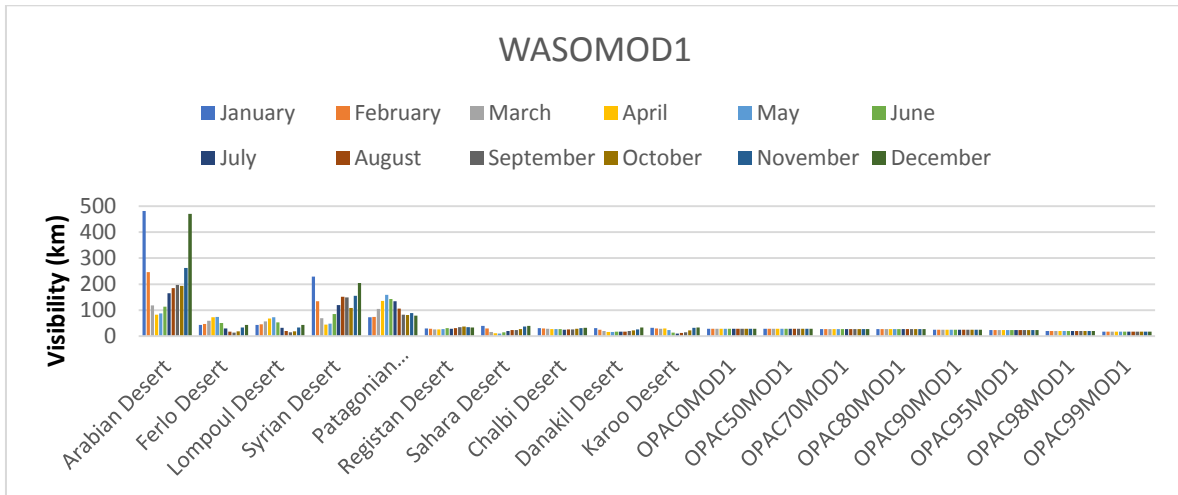
Fig. 1a. Visibility plot for OPAC and MEERA-2 (WASO Model1) at 550nm
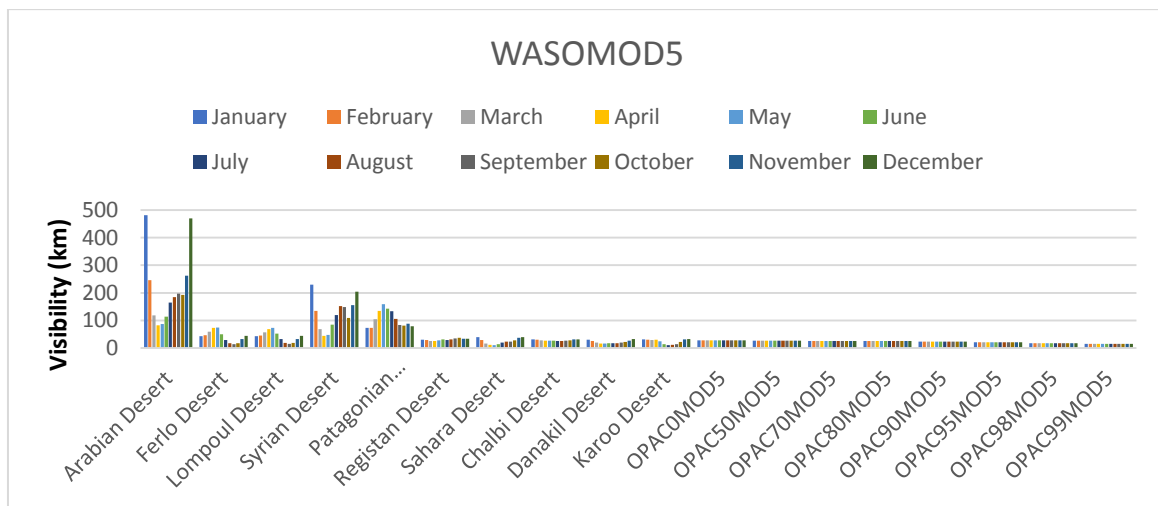

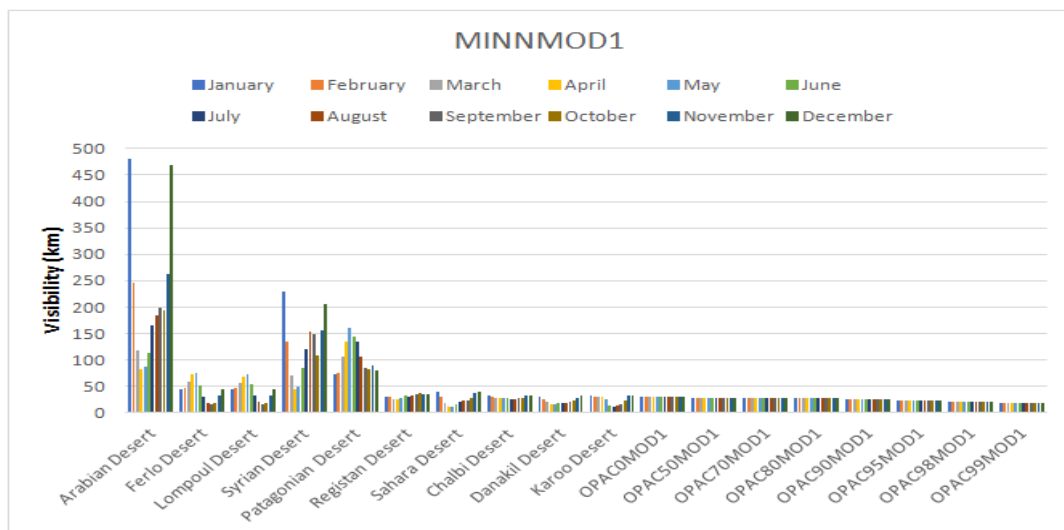**Fig.1b. Visibility plot for OPAC and MEERA-2 (WASO Model5) at 550nm**

Fig. 1c. Visibility plot for OPAC and MEERA-2 (MINN Model1) at 550nm
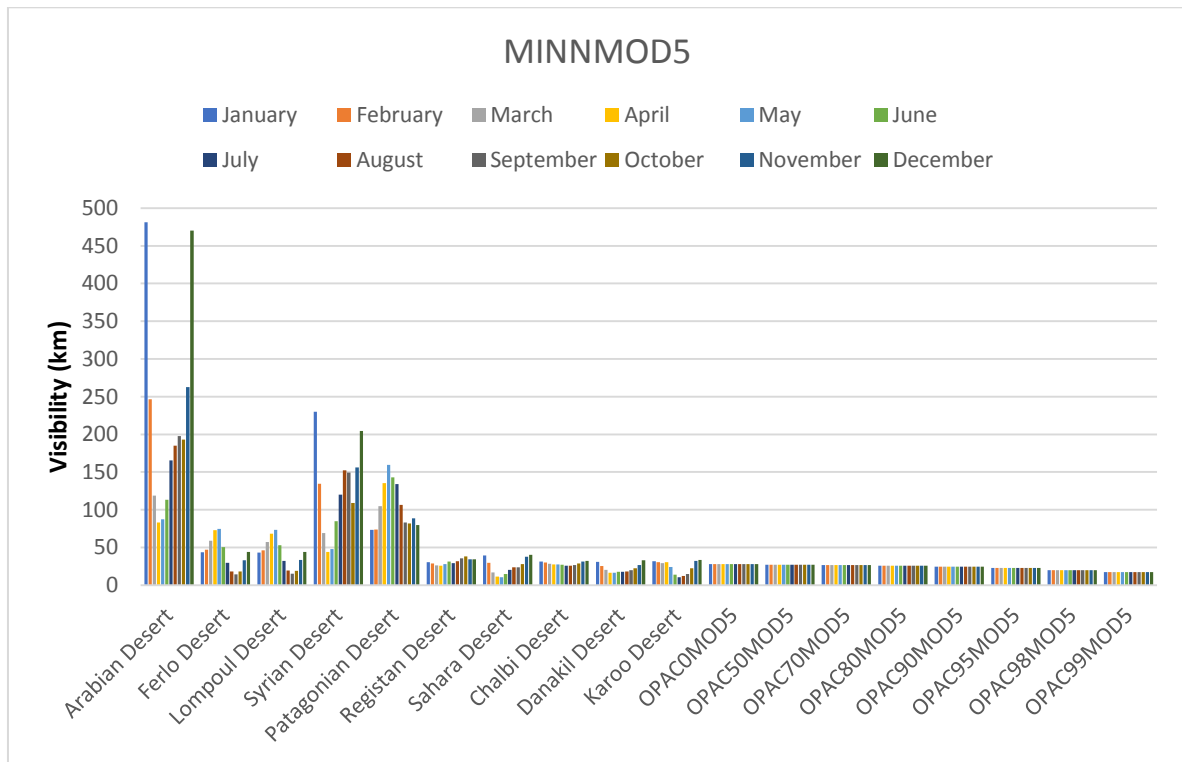
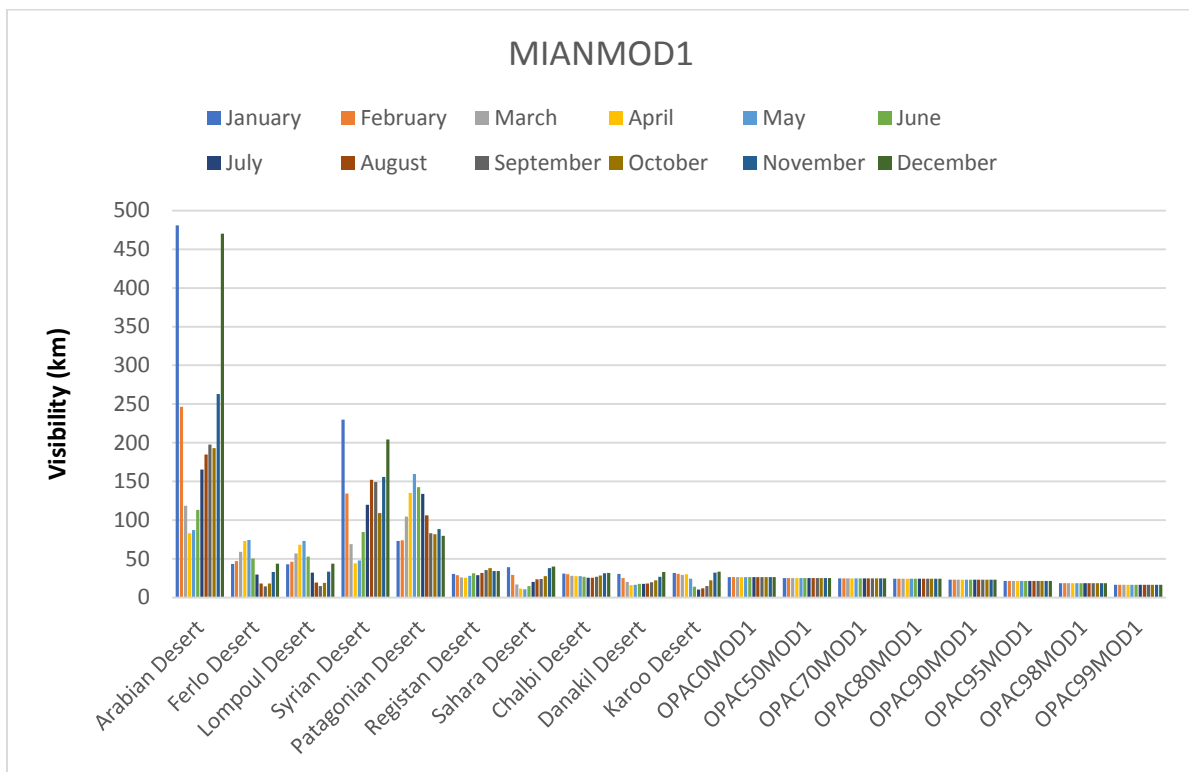**Fig. 1d. Visibility plot for OPAC and MEERA-2 (MINN Model5) at 550nm**

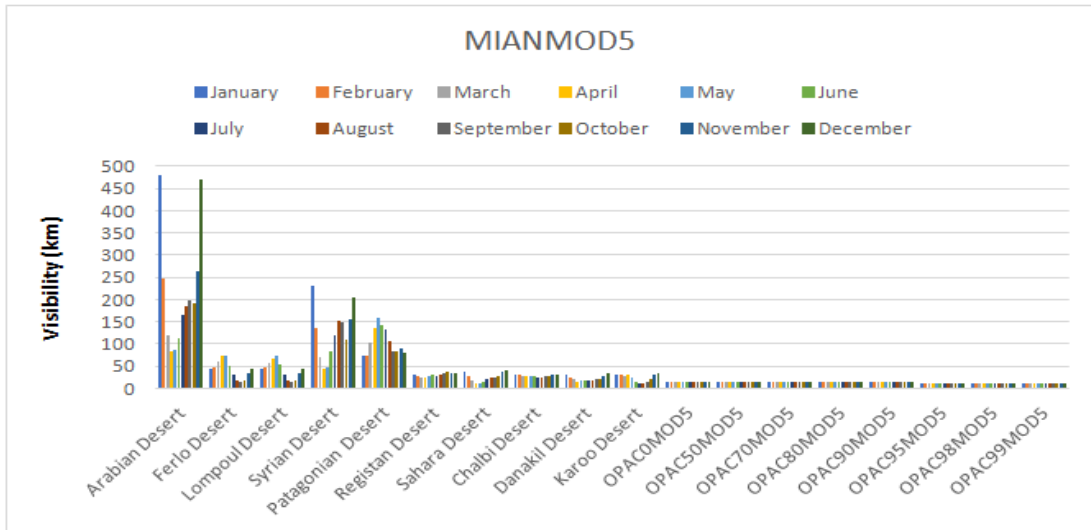**Fig. 1e. Visibility plot for OPAC and MEERA-2 (MIAN Model1) at 550nm**

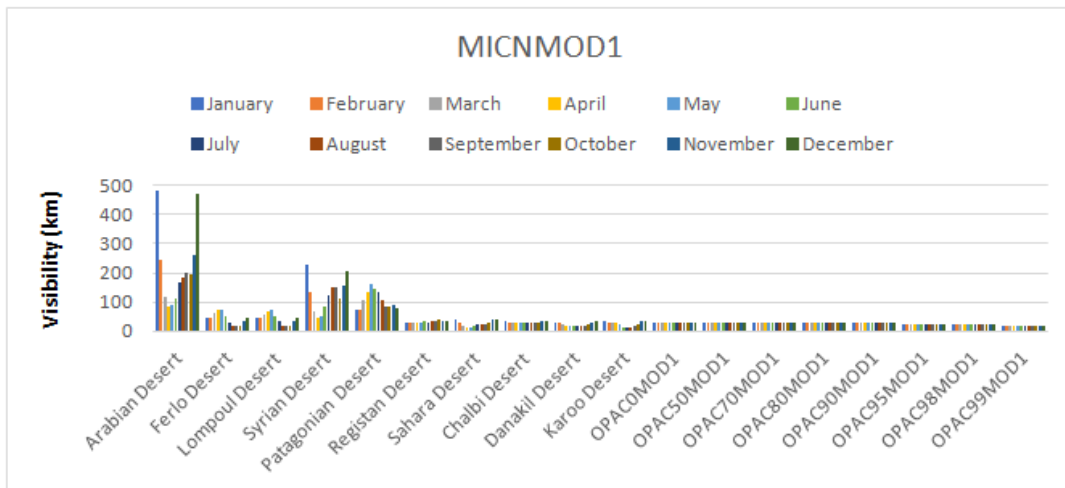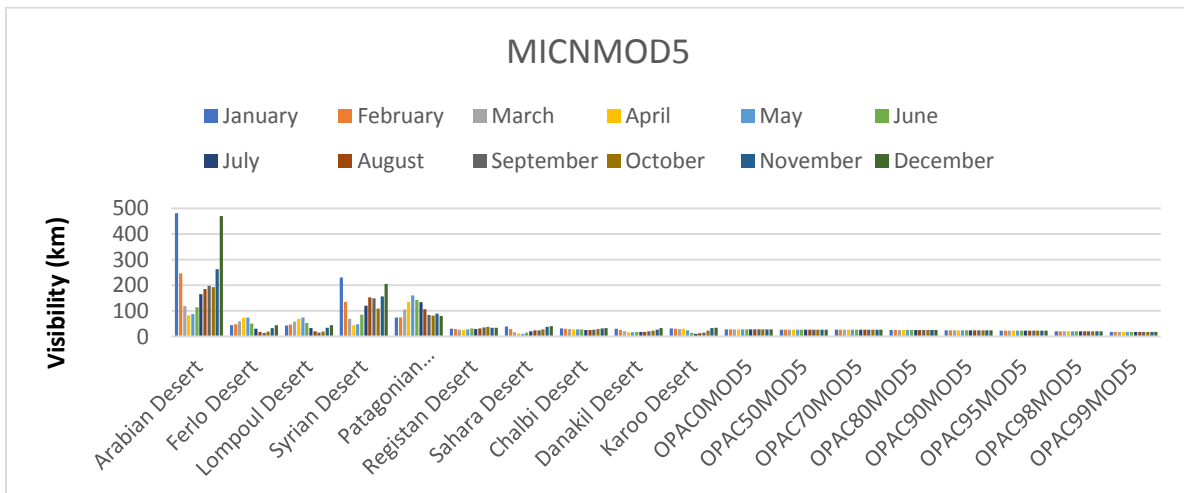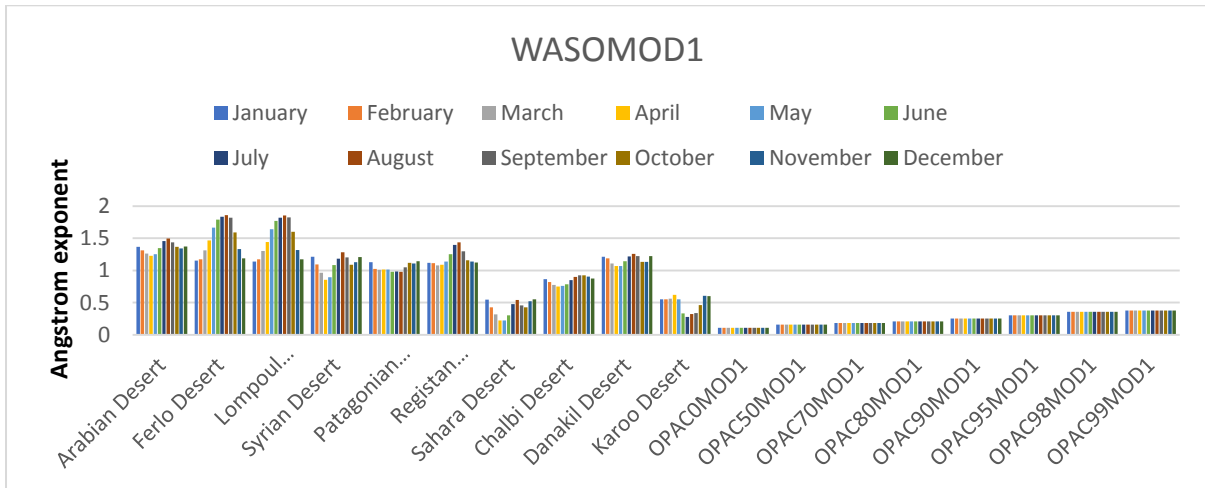**Fig. 1f. Visibility plot for OPAC and MEERA-2 (Model5) at 550nm**

Fig. 1g. Visibility plot for OPAC and MEERA-2 (MICNModel1) at 550nm

Fig. 1h. Visibility plot for OPAC and MEERA-2 (Model5) at 550nm

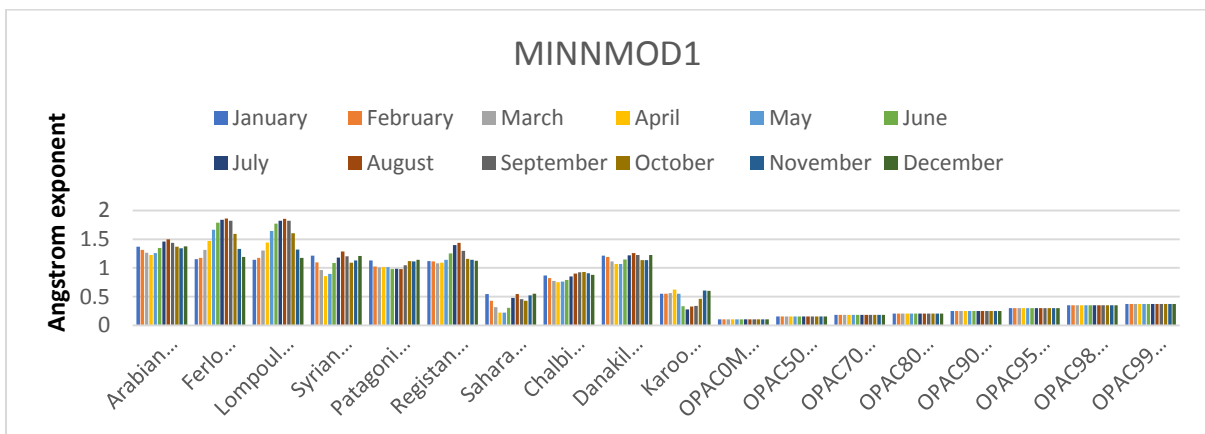**Fig. 2a. Angstrom exponent plot for OPAC and MEERA-2 (Model1) at 550nm**
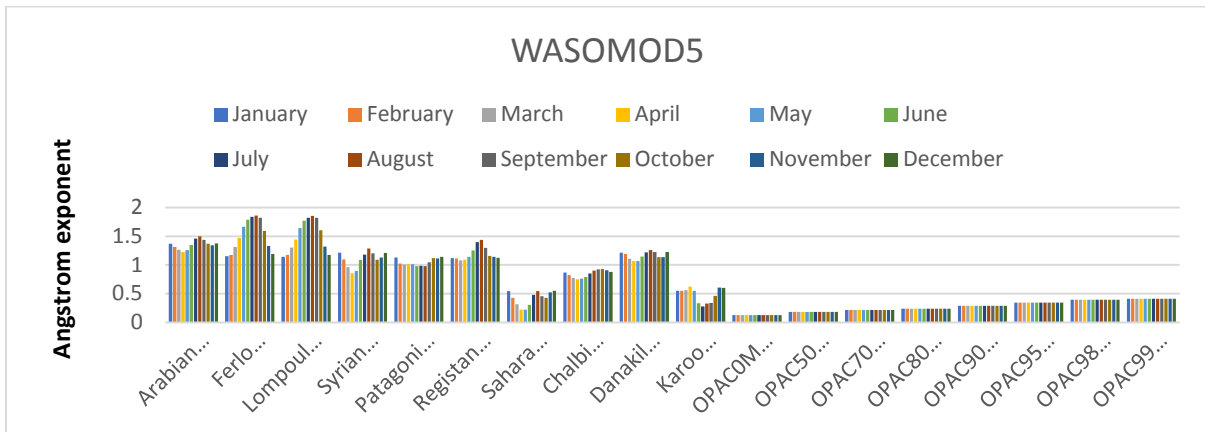
Fig. 2b. Angstrom exponent plot for OPAC and MEERA-2 (Model5) at 550nm

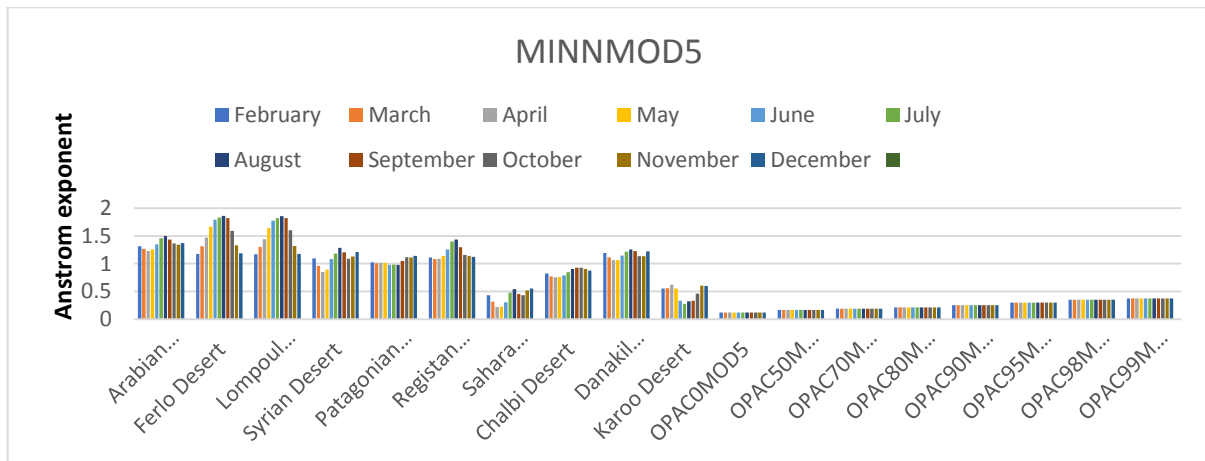**Fig. 2c. Angstrom exponent plot for OPAC and MEERA-2 (Model1) at 550nm**

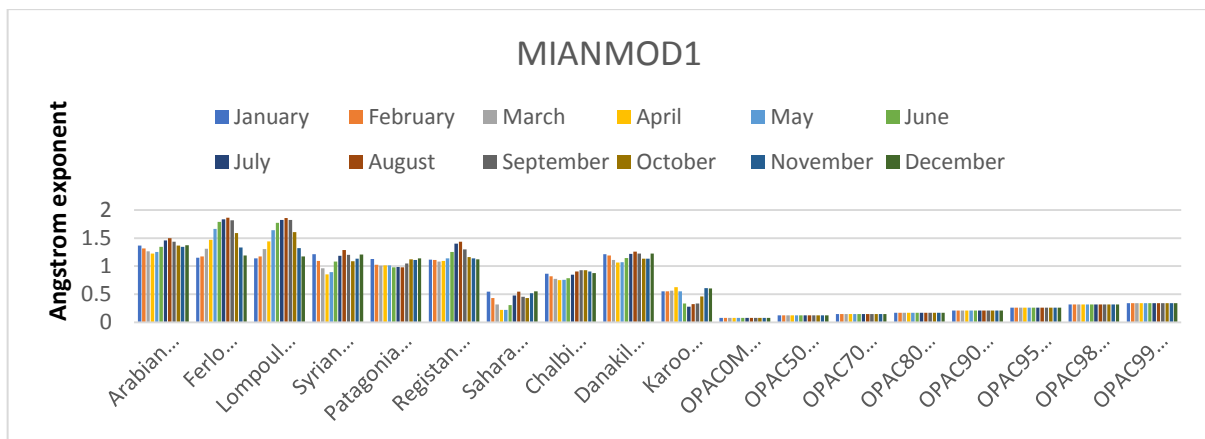**Fig. 2d. Angstrom exponent plot for OPAC and MEERA-2 (Model5) at 550nm**

Fig. 2e. Angstrom exponent plot for OPAC and MEERA-2 (Model1) at 550nm
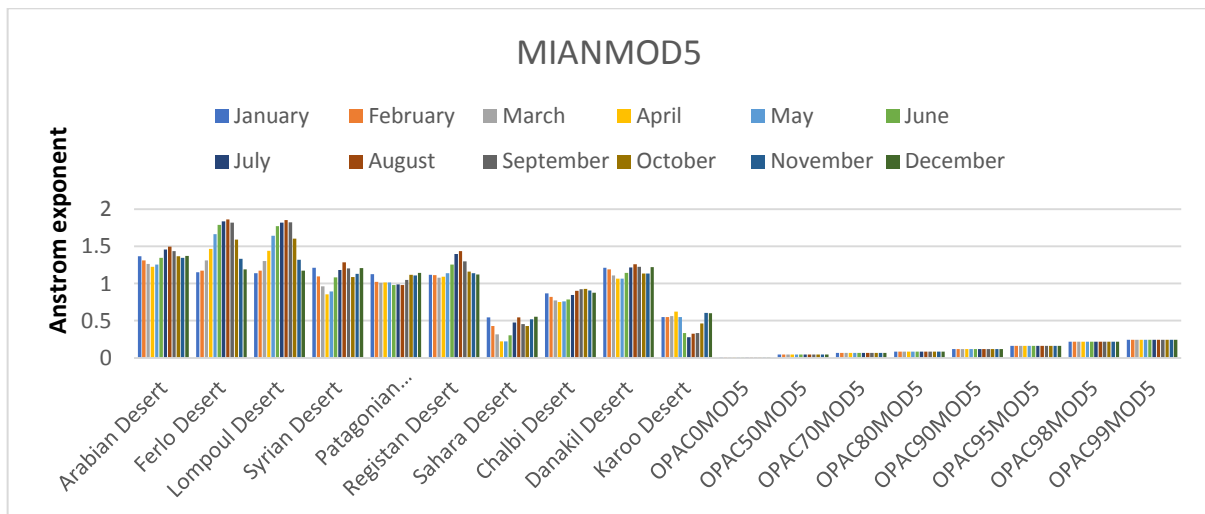

Fig. 2f. Angstrom exponent plot for OPAC and MEERA-2 (Model5) at 550nm

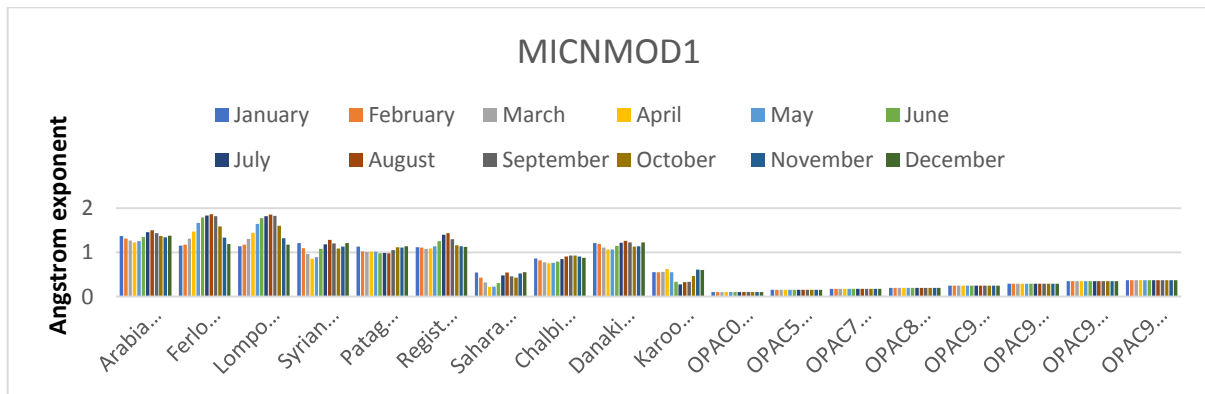**Fig. 2g. Angstrom exponent plot for OPAC and MEERA-2 (Model1) at 550nm**
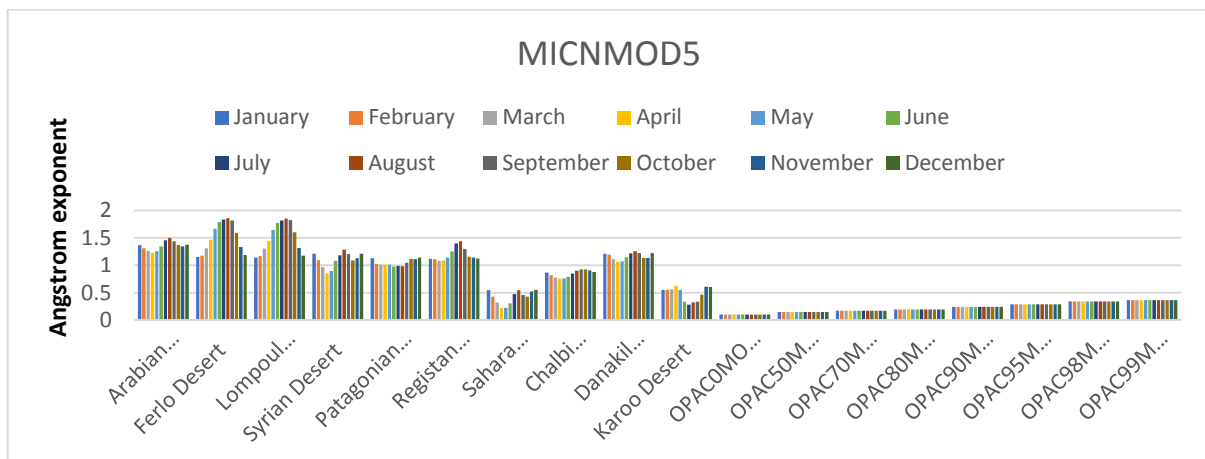

Fig. 2h. Angstrom exponent plot for OPAC and MEERA-2 (Model5) at 550nm

4. SUMMARY

The work used MEERA-2 model extracted angstrom exponent and extinction coefficient to validate results obtained from the analysis of data extracted from OPAC 4.0 in our previous work [10]. It was gathered from the results of the analysis that:

a) The R^2 values and the stationary R^2 for all the studied Deserts atmospheres show that the model under consideration is good and better than the baseline model.

b) The (β) level values of the model's significance are 0.0000 all through the ten studied deserts, which signifies that the model is significant.

c) The seasonality (δ) model's significance for all the studied deserts are not significant except for Ferlo and Lompoul deserts which are very significant.

d) From the plots, it can be said that the angstrom exponent (α) for both MEERA-2 model and OPAC 4.0 shows some agreements as they show same mode of variation over the studied period for (MEERA-2) and across the models for OPAC 4.0.

e) Ferlo and Lompoul has the highest angstrom exponent (α) values (highest concentration of fine mode particles) followed by Arabian, Registan, Danakil, Chalbi, and Karoo deserts. Sahara has the least (α) values.

f) The months of August, September and November have the highest (α) values for MEERA-2 Model which means that the highest concentration of fine mode particles is found in the months mentioned above.

g) For all the four studied components, MIAN has the least values of angstrom exponent (α) and that (α) increases with the increase in relative humidity.

h) The values of the angstrom exponent (α) for MEERA-2 model is higher than that of

OPAC 4.0 except for Sahara and Karoo Deserts for the period of (May, June, July and August) and (June, July, August, September, October and November) respectively.

i) The arabian, Syrian and Patagonian deserts have the highest visibility (km) for the months of January, February, June, November and December respectively.

j) The visibility decreases with in RH across the models and the studied components.

k) MIAN component has the least visibility for both MEERA-2 model and OPAC 4.0.

l) Some of the deserts (Ferlo, Lompoul, Registan, Sahara, Chalbi, Danakil and Karoo) follows the mode of changes in visibility with OPAC except for the months of May, June, July, August and September.

5. CONCLUSION

Based on the results obtained from the analysis of the data extracted from both MEERA-2 model and OPAC 4.0, it can be concluded that the angstrom exponent (α) for MEERA-2 model is greater than 1, (which signifies the dominance of fine mode particles) for all the Deserts atmosphere except for Chalbi (0.845), Karoo (0.482) and Sahara (0.417) deserts which have (α) values less than 1 (which shows the dominance of coarse mode particles), But MEERA-2 model still has the highest angstrom exponent value, higher than that of OPAC. It can say that MEERA-2 model predicted that it is possible for some deserts Atmosphere to have the dominance of fine mode particles over coarse mode particles. From the results of the investigation (time series analysis), it was found that the models are highly significant except for Ferlo and Lompoul deserts. It can also be concluded that, the significance for all the levels is very high, this shows that the aerosols distribution fluctuates around a reasonable mean. The MEERA-2 visibility is higher than that of the four OPAC 4.0 components (WASO, MINN, MIAN and MICN) respectively. The investigation further revealed that the Arabian, Syrian and Patagonian deserts have the highest visibility (km) for months of January, February, June, November and December. Mineral accumulation mode component (MIAN) has the least of the visibility (km) when compared to both MEERA-2 model with OPAC 4.0. the plots of visibility further showed that Ferlo, Lompoul, Registan, Sahara, Chalbi, Danakil and Karoo desert have almost same visibility values and follows almost the same trend except for the months of May, June, July, August and September.

COMPETING INTERESTS

Authors have declared that no competing interests exist.

REFERENCES

1. Renard JB, et al. In situ measurements of desert dust particles above the western Mediterranean Sea with the balloon-borne Light Optical Aerosol Counter/sizer (LOAC) during the ChArMEx campaign of summer 2013. Atmospheric Chemistry and Physics. 2018;18(5):3677-99.
DOI: 10.5194/acp-18-3677-2018.

2. Alessandrini ER, Stafoggia M, Faustini A, Gobbi GP, Forastiere F. Saharan dust and the association between particulate matter and daily hospitalisations in Rome, Italy. Occupational and environmental medicine. 2013;70(6):432-4.
DOI: 10.1136/oemed-2012-101182.

3. Ou Y, Li Z, Chen C, Zhang Y, Li K, Shi Z, Dong J, Xu H, Peng Z, Xie Y, Luo J. Evaluation of MERRA-2 Aerosol Optical and Component Properties over China Using SONET and PARASOL/GRASP Data. Remote Sensing. 2022 Feb 9;14(4):821.
DOI: 10.3390/rs14040821.

4. Yerima SU, Abdulkarim UY, Tijjani BI, Gana UM, Sani M, Aliyu R. Analysis of the impact of relative humidity and mineral accumulation mode aerosols particle concentration on the visibility and particle size distribution of desert aerosols. Int. J. Sci. Eng. Res. 2021;12(4):929–943.

5. Tijjani BI. The effect of soot and water soluble on the hygroscopicity of Urban Aerosols. Adv. Phys. Theor. Appl. 2013;26(1):52–73. [Online].
Available: www.iiste.org.

6. Neophytou AM, Yiallouros P, Coull BA, Kleanthous S, Pavlou P, Pashiardis S,

Dockery DW, Koutrakis P, Laden F. Particulate matter concentrations during desert dust outbreaks and daily mortality in Nicosia, Cyprus. Journal of Exposure Science & Environmental Epidemiology. 2013;23(3):275-80.
DOI: 10.1038/jes.2013.10.

7. Venero-Fernández SJ. Saharan dust effects on human health: a challenge for Cuba's researchers. MEDICC Review. 2016;18:32-4.
DOI: 10.37757/mr2016.v18.n3.8.

8. Rocha-lima A, et al. A detailed characterization of the Saharan dust collected during the Fennec campaign in 2011 : In situ ground-based and laboratory measurements. 2018;1023–1043.

9. Yerima SU, et al. Analysis of the impact of relative humidity and mineral nuclei mode aerosols particle concentration on the visibility of desert aerosols. 2021;8(1):114–131.

10. Yerima SU, Tijjani BI, Gana UM. Impacts of the variations of aerosols components and relative humidity on the visibility and particles size distribution of the desert atmosphere. 2021;4(3):42–65.
DOI: 10.9734/AJR2P/2021/v4i330146.

11. Abdulkarim UY, Yerima SU, Tijjani BI, Gana UM, Sani M. The effect of varying soot concentration and relative humidity on visibility and particle size distribution in urban atmosphere. 2021;8(1):83–101.

12. Maring H, Savoie DL, Izaguirre MA, Custals L, Reid JS. Mineral dust aerosol size distribution change during atmospheric transport. Journal of Geophysical Research: Atmospheres. 2003;108(D19).
DOI: 10.1029/2002jd002536.

13. De Longueville F, Ozer P, Doumbia S, Henry S. Desert dust impacts on human health: an alarming worldwide reality and a need for studies in West Africa. International journal of biometeorology. 2013;57(1):1-9.
DOI: 10.1007/s00484-012-0541-y.

14. Kasten F. Visibility forecast in the phase of pre-condensation. Tellus. 1969;21(5):631–635.
DOI: 10.3402/tellusa.v21i5.10112.

15. Ginoux P, Prospero JM, Gill TE, Hsu NC. M. Zhao. Global-scale attribution of anthropogenic and natural dust sources and their emission rates based on MODIS Deep Blue aerosol products. Rev. Geophys. 2012;50(3).

DOI: 10.1029/2012RG000388.

16. Washington R, Todd M, Middleton NJ, Goudie AS. Dust-storm source areas determined by the total ozone monitoring spectrometer and surface observations. Annals of the Association of American Geographers. 2003;93(2):297-313.
DOI: 10.1111/1467-8306.9302003

17. Akpootu DO, Momoh M. The ångström exponent and turbidity of soot component in the radiative forcing of urban aerosols. Nigerian Journal of Basic and Applied Sciences. 2013 Jun 14;21(1):70-8.
DOI: 10.4314/njbas.v21i1.11.

18. Shaik KS. Atmospheric propagation effects relavant to optical communications. Commun. Syst; 1988.

19. Mallone S, Stafoggia M, Faustini A, Gobbi GP, Marconi A, Forastiere F. Saharan dust and associations between particulate matter and daily mortality in Rome, Italy. Environmental health perspectives. 2011;119(10):1409-14.
DOI: 10.1289/ehp.1003026.

20. Wilson GT. Time series analysis: Forecasting and Control, 5th Edition, by George E. P. Box, Gwilym M. Jenkins, Gregory C. Reinsel and Greta M. Ljung. Published by John Wiley and Sons Inc., Hoboken, New Jersey. 712. ISBN: 978-1-118-67502-1. J. Time Ser. Anal. 2015;37(5):709–711,
DOI: 10.1111/jtsa.12194.

21. Tsilimigras P. On the applicability of the Roothaan-Bagus procedure. Chemical Physics Letters. 1971;11(1):99-100.
DOI: 10.1016/0009-2614(71)80541-9.

22. Charlson RJ. Current Research. 1969;3(10):913–918.

23. Ischult M. Hess, Koepke P. Optical properties of aerosols and clouds: The software package OPAC. 1998;831–844.

24. Moorthy KK, Saha A, Prasad BSN, Niranjan K, Jhurry D, Pillai PS. Aerosol optical depths over peninsular India and adjoining oceans during the INDOEX campaigns: Spatial, temporal, and spectral characteristics. J. Geophys. Res. Atmos. 2001;106(D22):28539–28554.
DOI: 10.1029/2001JD900169.

25. Singh S, Nath S, Kohli R, Singh R. Aerosols over Delhi during pre-monsoon months: Characteristics and effects on surface radiation forcing. Geophysical Research Letters. 2005;32(13).
DOI: 10.1029/2005GL023062.

26. Koschmieder EL. Symmetric circulations of planetary atmospheres. InAdvances in Geophysics 1978;20:131-181. Elsevier. DOI: 10.1016/S0065-2687(08)60323-4.

27. Mary E. Dzaugis, Arthur J. Spivack, S. D'Hondt, NASA Public Access. AIMS Geosci. 2017;3(2):163–186.

DOI: 10.1175/JCLI-D-16-0609.1.The.

28. Koepke P, Gasteiger J, Hess M. Technical Note: Optical properties of desert aerosol with non-spherical mineral particles: Data incorporated to OPAC. Atmos. Chem. Phys. 2015;15(10):5947–5956. DOI: 10.5194/acp-15-5947-2015.

Peer-review history:
The peer review history for this paper can be accessed here:
https://www.sdiarticle5.com/review-history/87931